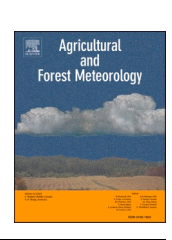
FISEVIER

Contents lists available at ScienceDirect

# Agricultural and Forest Meteorology

journal homepage: www.elsevier.com/locate/agrformet



# Importance of measured transpiration fluxes for modelled ecohydrological partitioning in a tropical agroforestry system

Christian Birkel <sup>a,b,c,\*</sup>, Saul Arciniega-Esparza <sup>d</sup>, Marco P. Maneta <sup>e</sup>, Jan Boll <sup>f</sup>, Jamie Lee Stevenson <sup>b</sup>, Laura Benegas-Negri <sup>c</sup>, Dörthe Tetzlaff <sup>g,h</sup>, Chris Soulsby <sup>b</sup>

- <sup>a</sup> Water and Global Change Observatory, Department of Geography, University of Costa Rica, San Jose, Costa Rica
- <sup>b</sup> Northern Rivers Institute, School of Geosciences, Aberdeen, Scotland, United Kingdom
- c Watershed, Water security and Soil Unit, CATIE, Turrialba, Costa Rica
- d Hydrogeology Group, Faculty of Engineering, Universidad Nacional Autónoma de México, Mexico City, Mexico
- Regional Hydrology Lab, University of Montana, Missoula, USA
- f Water and Environmental Laboratory, Washington State University, Pullman, USA
- g Department of Ecohydrology, Leibniz Institute of Freshwater Ecology and Inland Fisheries, Berlin, Germany
- <sup>h</sup> Department of Geography, Humboldt University Berlin, Berlin, Germany

#### ARTICLE INFO

#### Key words: Ecohydrology Water partitioning Conceptual modelling Transpiration Tropics

#### ABSTRACT

Evaporation (E) and transpiration (Tr) are the key terrestrial water fluxes to the atmosphere and are highly sensitive to land cover change. These ecohydrological fluxes can be measured directly only at small scales, such as individual plants or under laboratory experiments. Modelling is needed to upscale E and Tr estimates to plot, hillslope and catchment scales. However, model-derived ecohydrological water partitioning of E and Tr can be ambiguous, particularly when models are trained using hydrometric data and soil moisture. To test the influence of different types of data (i.e., sap flux-derived Tr, Eddy Covariance-derived actual evapotranspiration (AET) and measured soil water (SW)) on model calibration and subsequent water partitioning, we developed the lowparameter plot scale ecohydrology model EcoHydroPlot applied to a data-rich experimental agroforestry plot in humid tropical Costa Rica. The model was able to simulate SW well when calibrated with any data type, but large differences emerged in the E and Tr flux partitioning. Using only hydrometric data for calibration resulted in parameter configurations that produced greater E over Tr fluxes (Tr/AET < 0.5). The opposite was seen for model calibration using Tr data (median Tr simulations with KGE > 0.6), resulting in Tr/AET ratios close to the observed ~0.9. Further, using all measurements simultaneously (including AET, SW and Tr) did not improve simulated water partitioning. We only found small differences between sun and shade locations with slightly greater average shaded coffee transpiration at the expense of lower upper SW, higher deeper SW and less groundwater recharge compared to sun exposed coffee. This work can inform measurement priorities for applications with relatively simple conceptual ecohydrology models and emphasizes the importance of transpiration estimates for model calibration beyond tropical environments.

#### **Key points**

- Ecohydrology model simulates water partitioning in tropical coffee plantation
- Water balance reapportionment was sensitive to calibration targets
- Transpiration data needed in calibration to capture green water

# contribution to total AET

- Including all calibration targets increase model performance and uncertainty  $% \left( 1\right) =\left( 1\right) \left( 1\right) \left($
- Shaded coffee transpires more and recharges less water compared to sun plot

<sup>\*</sup> Corresponding author at: Water and Global Change Observatory, Department of Geography, University of Costa Rica, San Jose, Costa Rica. E-mail address: christian.birkel@ucr.ac.cr (C. Birkel).

#### Data availability

Data will be made available on request.

#### 1. Introduction

The tropics have experienced accelerated change in land cover (e.g., Meli et al., 2017), modifying the partitioning of rainfall into evaporation (E) and transpiration (Tr), infiltration and groundwater recharge, as well as runoff dynamics (Grip et al., 2005). Large scale impacts include altered soil-vegetation-atmosphere feedbacks, such as reduced moisture recycling and other rainfall-producing mechanisms due to forest cover loss (te Wierik et al., 2021). However, quantifying how much land cover change impacts the hydrological cycle strongly depends on measurements from monitoring networks, which are declining in many places, particularly in the tropics (Wohl et al., 2012). Nonetheless, many measurement techniques used to estimate Tr (e.g., Eddy Covariance and sap flux) are based on point measurements and need upscaling to larger areas, which inevitably results in considerable assumptions and uncertainty (Ford et al., 2007). Despite these many uncertainties, larger scale remote sensing and modelling are usually the most appropriate methods to indirectly estimate plot and catchment scale ecohydrological water partitioning into "green" water losses (i.e., E and Tr) and "blue" water fluxes (i.e., groundwater recharge and runoff). In addition to ecohydrological modelling, stable isotopes have also been used to analytically derive water balance components (Jasechko et al., 2013). However, stable isotope-based estimates of ecohydrological water partitioning often do not agree with those obtained from hydrological models and result in a wide, and climate-dependant, range of Tr/AET (Actual Evapotranspiration) ratios from 0.2 to close to 1 (Schlesinger and Jasechko, 2014). In general, ecohydrological modelling tends to produce lower Tr/AET estimates with greater emphasis on E fluxes relative to Tr, particularly if compared to stable isotopes (Schlesinger and Jasechko, 2014). The latter arises from model parameter uncertainty and lacking ecohydrological data to constrain models. Studies in the tropics have shown the largest Tr fluxes worldwide, with stable isotope-based estimates reaching Tr/AET ratios close to 1, whereas hydrological modelling has produced estimates closer to 0.5 (Arciniega et al., 2022).

Differences in how ecohydrological models partition water are also related to inherent uncertainties and how simple or complex a soilvegetation-atmosphere model should be (Franks et al., 1997). Many published ecohydrological models are distributed in space and process-based (e.g., EcH2O, RHESSys, STARR) and require a lot of data to drive them (Maneta and Silvermann, 2013; Tague and Band, 2004; van Huijgevoort et al., 2016, respectively). However, in most applications detailed and spatially-distributed data of, in particular, vegetation and soil physical characteristics are often limited or unavailable, which is a reason simpler ecohydrological models are still popular. These simpler models are often very successful at capturing dominant processes and can be applied more widely to estimate the water "footprint" of different land uses and vegetation types (Stevenson et al., 2023). Additionally, there is still a need to understand effects of different calibration constraints on quantifying key processes and fluxes in ecohydrological models (Kuppel et al., 2018; Douinot et al., 2019; Schreiner-McGraw et al., 2022).

Current patterns of land use conversion in the humid tropics, coupled with projected climate change, create an urgent need for an evidence base to inform policy directed to more sustainable integration of land and water management (Griscom et al., 2017). Here, reliable ecohydrological models to quantify water use by different land use types could provide such evidence-based information for decision-making (e.g., Smith et al., 2021). For example, enhanced understanding of the trade-offs between crop and timber production and water availability for

other services (e.g., groundwater recharge, sustaining river flows and linked water quality) is crucial in better implementing ecohydrological goals into, for example, payment for ecosystem services schemes (Birkel et al., 2012). In particular, high value export crops (e.g., coffee, fruit) need to be considered due to their substantial contributions to national economies of tropical countries (Ovalle-Rivera et al., 2015). For example, possible decreased coffee productivity due to climate change is alarming (Pham et al., 2019) and likely related to more biodiversity loss (Philpott et al., 2008). Spatial shifts in Arabica coffee producing regions are also expected (Ovalle-Rivera et al., 2015) with concerns over seemingly less resistant Robusta coffee (Kath et al., 2020). In the context of climate change, shade coffee production of planted trees in between coffee hedgerows has since been seen as a viable alternative with hydrological (in the context of reduced AET) and soil structural and biogeochemical benefits over coffee directly exposed to the sun particularly in Costa Rica (Siles et al., 2010; Harmand et al., 2007).

In this paper, we address the issue of simulating ecohydrological water partitioning with a relatively simple conceptual ecohydrological model set up at the plot-scale for the humid tropics applied to a well-instrumented agroforestry (sun coffee vs shade coffee covered by trees) experiment in eastern humid tropical Costa Rica, where measurements of most components of the hydrological cycle are available for calibration and validation. We tested the model with different calibration targets of measured soil water (SW), transpiration (Tr) and actual evapotranspiration (AET) and evaluated which data type results in the most plausible simulated ecohydrological water partitioning. We hypothesized that including more calibration targets would result not only in the most optimal model performance but also in the best partitioning of E and Tr fluxes.

The specific objectives were to:

- (i) Set up a parsimonious ecohydrology model for simulation of 1D fluxes at the plot-scale in a tropical coffee plantation.
- (ii) Test different calibration targets and their impact on the ecohydrological water partitioning using a flux mapping approach.
- (iii) Evaluate which type of data are most useful for calibrating the ecohydrology model focusing on water partitioning under contrasting land use (e.g., coffee vs coffee under shade trees) in a context of land management.

# 2. Revisiting the Mejias coffee-flux observatory

The Mejias catchment ( $\sim$ 0.9 km<sup>2</sup>) and a plot-scale experiment started in 2008 as the Coffee-Flux agroforestry research project by CIRAD (Centre de coopération International en Recherche Agronomique pour le Developpément) and in collaboration with CATIE (Centro Agronómico Tropical de Investigación y Enseñanza) to assess, amongst many ecohydrological issues, how shade trees would impact coffee production (Roupsard et al., 2016). The experiment was part of FLUXNET (Baldocchi et al., 2001) and was based in an active coffee-producing farm in Aguiares near the city of Turrialba on the Caribbean slope of Costa Rica at an altitude of 1040m.a.s.l. (Fig. 1). This region is characterized by annual rainfall above 2000mm with little seasonality and virtually no thermal intra-annual oscillations (Fig. 2a, b, c, d). The mean annual temperature at the Mejias site is around 19.6°C. The Mejias plot consisted of a meteorological tower (precipitation (P), radiation, temperature (T), relative humidity (RH), wind speed) with Eddy Covariance measurements of gas exchanges estimating the complete energy balance and ecosystem productivity (Charbonnier et al., 2013). The research team instrumented soil profiles in sun-exposed and shaded areas with volumetric soil water content (SW) sensors to a total depth of 3.5m close to the tower. Shaded coffee (Coffea arabica L., dwarf var. Caturra) under Erythrina poepiggiana trees and sun exposed coffee plants were equipped with sap flux sensors (Dynamax) and manual leaf-area-index (LAI) measurements were made systematically in the sun and shade locations (Fig. 1). Erythrina poepiggiana was planted with a low density (7.4 trees

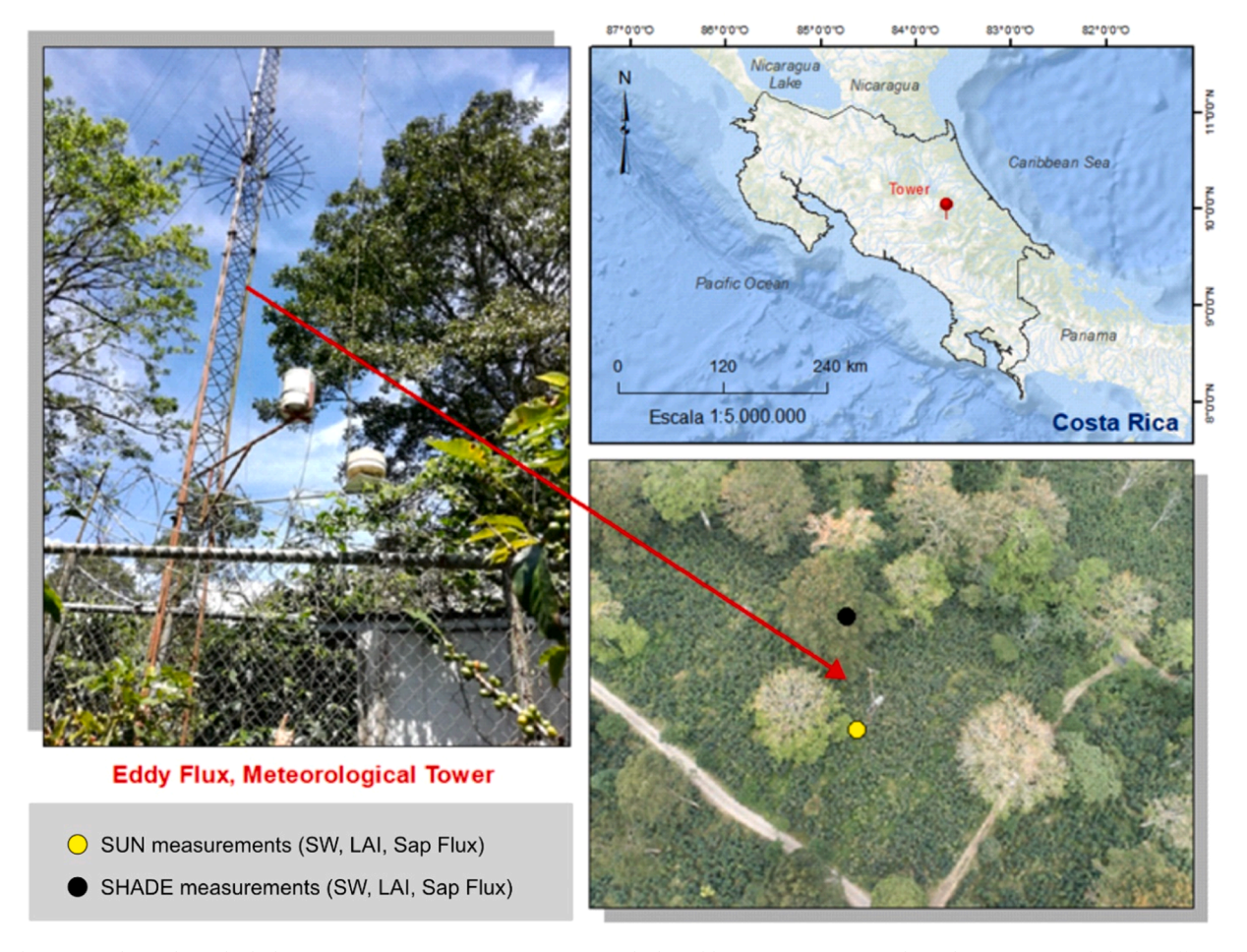


Fig. 1. The Mejias plot-scale ecohydrology experiment in eastern Costa Rica with the Eddy Covariance meteorological tower, sun and shade coffee monitoring locations of SW and LAI in the regional context of Central America.

ha<sup>-1</sup>) and were left freely-growing, which resulted in tall (>20m) but sparse trees covering the entire plantation. Initially, Arabica coffee plants were established with a density of 6300 seedlings ha<sup>-1</sup> and were intensively managed with pruning according to plant age and fertilizer application. The 1.6ha plot around the meteorological tower included 14 trees that provided a canopy cover of up to 30% of the plot area.

The soil characteristics correspond to loamy sands of volcanic (shallow intrusive volcanic rock) origin (Andosol) with high saturated hydraulic conductivity (>100m  $h^{-1}$ ) and high infiltration capacities (Benegas et al., 2014). The soils in the study area also exhibit a relatively high fraction of stones of a colluvial origin, likely from a large-scale paleo-landslide, mixed with volcanic flows, lahars, agglomerates and ashes. The soil characteristics of the study plot favour vertical hydrological fluxes coinciding with water balance measurements and modelling, which found minor overland flow contributions (<4%) to streamflow in the Mejias catchment (Gomez-Delgado et al., 2011).

#### 3. Data and methods

The data sets used here are extensively described in Gomez-Delgado et al. (2011), Charbonnier et al. (2013), Taugourdeau et al. (2014) and cover the study period from January 2010 until December 2013 as the most consistent. For all inputs we used hourly-averaged data from measurements conducted at 15-min intervals. Minor model input data gaps were linearly interpolated, but the period from 2010 to 2013 showed a consistent set of data with less than 1% missing values. Gaps in AET, Tr and SW were generally not filled when used for model evaluation purposes.

# 3.1. Model forcing and evaluation data

#### 3.1.1. Model forcing

Precipitation, potential reference evapotranspiration (PET) and a continuous hourly time series of LAI were used to force the model. Gross P was measured with a tipping bucket gauge (0.2mm) mounted on the meteorological tower at 3m height along with all other meteorological measurements except the wind speed sensor which was mounted at 10m above the surface and orientated toward the study plot (Charbonnier et al., 2013). The meteorological variables were used to estimate PET with the FAO Penman-Monteith Equation (Allen et al., 1998). The hourly, cover-weighted LAI time series for sun (coffee) and shade (coffee shaded by trees) locations in  $m^2 m^{-2}$  were linearly interpolated from weekly duplicate LAI2000 measurements (LI-COR, 1992) covering 14 transects to match natural phenological dynamics related to climate and agricultural practice such as pruning and fertilizing coffee plants (Taugourdeau et al., 2014). The two LAI2000 instruments were matched prior to each measurement under diffuse light conditions according to the LI-COR standard protocol. Arabica coffee phenological cycles generally cover two years with a typical leaf lifespan of 1.5 years. The overall average measured LAI was  $3.78 \,\mathrm{m}^2 \,m^{-2}$  with lower values during the drier months from January to April coinciding with pruning and higher LAI values over the wetter months from May to December also related to fertilizer application and harvest (Fig. 2i, j). Generally, the average interpolated LAI for shaded coffee is slightly lower (4.02 m<sup>2</sup>  $m^{-2}$ ) compared to the fully sun exposed coffee plants (4.2 m<sup>2</sup>  $m^{-2}$ ) but exceeds sun LAI at the beginning of the rainy months in May. The shade providing Erythrina trees shed their leaves in drier and slightly cooler

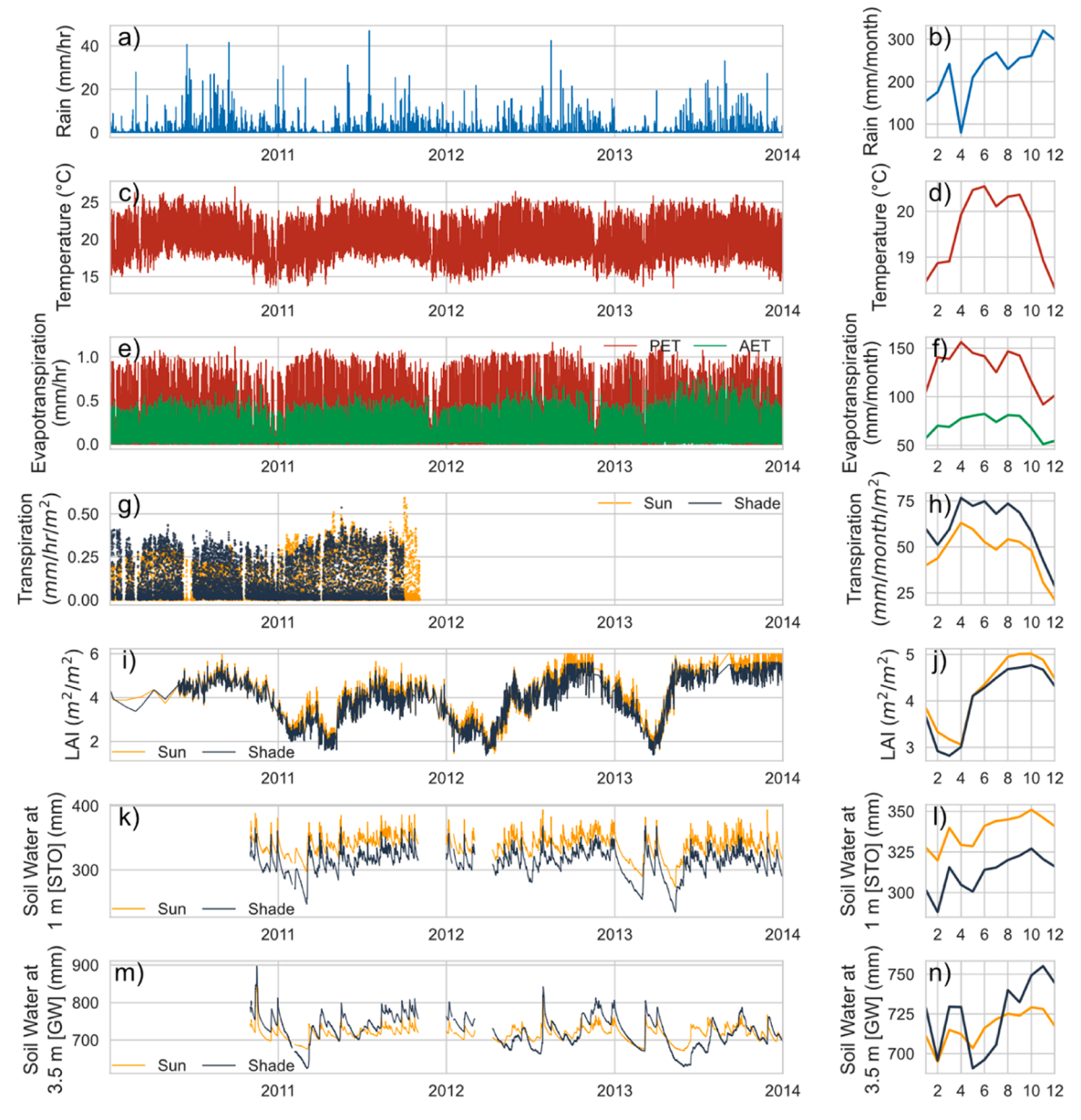


Fig. 2. (a, c, e, i, k, m) Hourly timeseries of forcing (rainfall, Leaf Area Index (LAI) and potential evapotranspiration (PET)) and observed data for evaluation (actual evapotranspiration (AET), soil water at 1m (STO) and soil water at 3.5m (GW)) of sun and shade locations at the Mejias plot from 2010 until 2014. b, d, f, h, j, l, n) mean monthly time series. Mean monthly transpiration time series for shadow and sun locations h) were averaged from available observations.

months and reached an LAI = 0 in mid-February synchronized with the coffee LAI minimum (Taugourdeau et al., 2014).

# 3.1.2. Evaluation data

The model evaluation used Eddy Covariance (EC) measured AET for the whole plot following the measurement and filtering procedure by Roupsard et al. (2006) from a tower elevation of 26m. The SW measurements used Campbell TDR probes at 10cm, 20cm, 50cm, and 90cm and were depth-integrated to 1m (STO). The SW measurements at 150cm, 200cm, 290cm, and 330cm were integrated to 3.5m depth for modelling purposes (GW). The SW measurements were presented by Benegas et al., (2014) and we based the depth integration from 0 – 100cm and 100 - 350cm on their rooting depth observations down to a depth of 3.5m with the highest root density in the first metre of soil. The sap flux probes (calibrated Dynamax devices using the method of Granier et al., 1996) were installed in six coffee plants in the sun and seven shaded coffee plants and in two trees. The sap flux variability amongst measured plants was characterized as the standard deviation around the

mean of  $0.77\pm0.198~{\rm dm^3~dm^{-2}~h^{-1}}$  for shade coffee plants and as  $0.808\pm0.141~{\rm dm^3~dm^{-2}~h^{-1}}$  for sun coffee plants over the measurement period of close to two years. Sap fluxes were converted into cover-weighted transpiration fluxes in mm  $h^{-1}$  using sapwood area measurements per plant (Leuning et al., 1995). The latter was then averaged to the sun and shade locations separately. The filtered AET measurements represent a whole plot estimate integrating over the coffee and shade tree plants in the study plot (see Charbonnier et al., 2013 and Roupsard et al., 2006 for details on EC data processing).

# 3.2. EcoHydroPlot model setup

The EcoHydroPlot model is a relatively parsimonious conceptual, plot-scale model set up to simulate ecohydrological water partitioning of E, Tr, and groundwater recharge, similar to Stevenson et al. (2023) (Fig. 3). The model runs on an hourly time step and uses precipitation, PET as forcing data, and LAI as an indicator of interception (D), with interception increasing proportionally with LAI. The non-linear

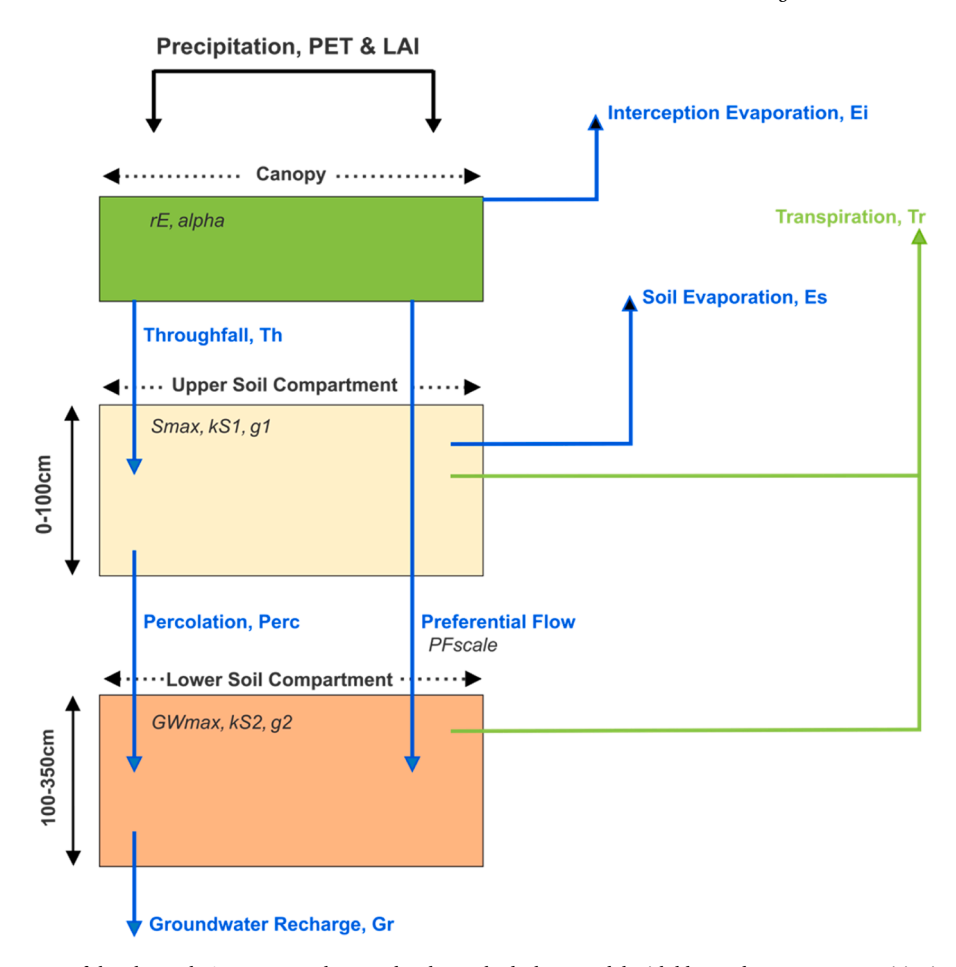


Fig. 3. Schematic model concept of the plot-scale 1D conceptual EcoHydroPlot ecohydrology model with blue and green water partitioning. Calibrated parameters in Italics are related to each model compartment (Table 2).

interception storage can lose water to the atmosphere via interception evaporation (Ei) at a rate given by PET if there is enough water available. The LAI is also used to calculate the Surface Cover Fraction (SCF) of the canopy using Beer's Law Eq. (1), which requires the calibration of a radiation extinction parameter (*rE*).

$$SCF[i] = 1 - \exp(rE \ LAI[i]) \tag{1}$$

The SCF and a calibrated interception threshold parameter ( $\alpha$ ) were used to calculate the maximum canopy interception storage (D; Eq. (2)) at each timestep (i). The SCF was also used to scale PET into a potential evaporation (Ep) and potential transpiration (Tp) component following Šimůnek et al. (2013) for an initial water partitioning.

$$D[i] = (\alpha \ LAI[i]) \left( 1 - \left( 1 \ \left/ \ \left( 1 + \left( \frac{SCF[i] \ P[i]}{\alpha \ LAI[i]} \right) \right) \right) \right) \right)$$
 (2)

We followed the premise that denser vegetation would transpire more water compared to less dense (< LAI) vegetation (Eqs. (3) and (4). Any depth of P in excess of D was routed to the upper soil compartment as throughfall ( $T_h$ ). Throughfall was summed to represent net precipitation (PN) after interception. For larger rain events > P90, we allowed a fraction of PN calculated with the calibrated parameter  $PF_{Scale}$  to directly reach the upper soil storage (STO) and subsequently the lower soil reservoir (GW). Such a preferential flow component was conceptualized based on the macropore rich soils and observed transient behaviour of the soil water (Fig. 2k, m).

$$SCF[i] = 1 - \exp(rE \ LAI[i])T_p[i] = SCF[i] \ PET[i]$$
 (3)

$$E_p[i] = (1 - SCF[i]) PET[i]$$
(4)

Overland flow was not observed at the plot site and, therefore, not used in the model. Furthermore, the flat topography limited lateral flows above the groundwater table, and therefore, the model represents exclusively vertical water fluxes. From the upper soil (STO), water can return to the atmosphere in form of soil evaporation (Es) and transpiration ( $\text{Tr}_{\text{upper}}$ ). Atmospheric water losses Es and  $\text{Tr}_{\text{upper}}$  are scaled using the calibration parameter Smax, which represents the maximum soil storage capacity (Eqs. (5) and (6)).

$$Tr_{Upper}[i] = T_p[i] \left( \frac{STO[i]}{S_{max}} \right)$$
 (5)

$$E_s[i] = (Ep[i] - Ei[i]) \left(\frac{STO[i]}{S_{max}}\right)$$
 (6)

Percolation (Perc) nonlinearly recharges the deeper soil layer (GW) according to Eq. (7) using the calibration parameters ks1 and g1 (Collenteur et al., 2021). Hereby, the parameter g1 determines how nonlinear the percolation flux will be and resorts to the linear case for g1=1.

$$Perc[i] = ks1 \left(\frac{STO[i]}{S_{max}}\right)^{g1} \tag{7}$$

The vegetation can also draw water for transpiration  $Tr_{lower}$  from the GW reservoir since roots were observed to a depth of 3m. The lower transpiration is scaled using a maximum groundwater storage capacity parameter GWmax Eq. (8).

$$Tr_{Lower}[i] = \left(T_p[i] - Tr_{Upper}[i]\right) \left(\frac{GW[i]}{GW_{max}}\right)$$
 (8)

The loss of water simulated from the deeper GW reservoir can therefore be considered representative of a nonlinear groundwater recharge (Gr) to the average water table at a depth of 5m using Eq. (9) with the calibrated parameters *ks2* and *g2*.

$$G_r[i] = ks2 \left(\frac{GW[i]}{GW_{max}}\right)^{g2} \tag{9}$$

The model was evaluated with data from measurements in the sun and shade of the experimental plot for comparison purposes (Fig. 2).

We initially ran the model 100,000 times using a Latin Hypercube Monte Carlo parameter sampling scheme (Soetaert and Petzoldt, 2010) with the widest physically feasible parameter ranges to constrain the model parameter ranges prior to calibration using multi-objective optimization. The constrained initial parameter ranges for model calibration (Table 2) were based on the best-performing (highest performance scores) 500 parameter sets in terms of SW (STO + GW), AET and Tr model performance determined using the modified Kling-Gupta efficiency (KGE) criterion (Kling et al., 2012).

# 3.3. Model calibration, evaluation, and uncertainty

The non-sorting genetic multi-objective calibration algorithm (NSGA2, Deb et al., 2002) was used with different calibration targets comparing model performance in relation to water partitioning. The calibration targets used measured SW, AET and Tr data in combination with the KGE criterion (Kling et al., 2012) and the mean absolute error (MAE). The calibration targets were applied to the shade and sun locations with varied LAI model inputs in the following combinations:

- Benchmark using all available targets for simultaneous calibration: KGE for SW, AET and Tr (SW-AET-Tr)
- (ii) KGE for SW and AET (SW-AET)
- (iii) KGE for SW and Tr (SW-Tr)
- (iv) KGE for SW(SW)
- (v) KGE and MAE for wholeplot AET (AET)
- (vi) KGE and MAE for Tr (Tr)

The NSGA2 algorithm was run with 500 parameter sets over 100 parameter generation permutations. The best-performing (highest KGE and MAE scores) final 500 parameter sets were subsequently used for model simulation, performance assessment and ecohydrological water partitioning. Model simulations were additionally evaluated using correlation coefficients (CC) and the root mean squared error (RMSE) criterion (R Core Team, 2022).

We conducted a parameter sensitivity ranking using LH—OAT (Latin Hypercube One-at-a-time; van Griensven et al., 2006) for the KGE performance criterion at the sun and shade locations gauging the impact of SW, AET and Tr on calibration and resulting flux simulations.

# 3.4. Water partitioning and flux mapping

The modelled fluxes were initially summed to annual values for water balance checks and in order to calculate water partitioning indices of Tr/AET and Tr/P. Simulated ecohydrological processes of Ei, Es, Tr and  $G_r$  were analysed using a flux mapping approach in form of ternary plots (Zhou et al., 2016; Khatami et al., 2019). This allowed us to visualize the relative contribution of each water loss simulated by the model compared to measured data of SW, AET and Tr using each calibration target.

# 4. Results

# 4.1. Plot-scale ecohydrological fluxes with a simple model

The study period from 2010 to 2013 was characterized by varied

climate conditions, including a wetter than normal 2010 (3316mm of annual rainfall) and a slightly drier than normal El Niño year with 2112mm of rainfall in 2012-2013 (Table 1). The latter dry conditions were reflected in a marked SW recession at the end of 2012 and the beginning of 2013 down to a depth of 3.5m (Fig. 2). The first metre of soil was characterized by transient and dynamic responses to rainfall with a slightly more attenuated response at depth which was independent of the sun or shade locations. However, the sun exposed location resulted on average in a slightly lower observed SW compared to the shade location. The overall soil water dynamics, including the peaks and drying events, were matched by all the model versions calibrated with any type of data. Here, we only show the benchmark calibration results (Fig. 4). Shifted peak simulations compared to the measured data were most likely the product of untraceable data errors in P input and/or the SW series. All SW simulations resulting from the different calibration targets were above KGE>0.6.

The AET and Tr simulations by all modelled calibration targets reproduced the observed diurnal cycle (Fig. 5 visualizes one exemplary month of hourly data). However, simulated differences emerged for different calibration targets that can be best visualized by the cumulative distributions for the whole simulation period in Fig. 5 with a wider spectrum for Tr simulations compared to AET independent of the sun or shade locations. Fine-scale details of small observed night-time Tr fluxes only at the shade location could not be reproduced by our simple model.

Comparing model performance (KGE, CC and RMSE criteria) for measured vs. simulated AET and Tr amongst the different calibration targets of the retained 500 best parameter sets (see full distribution of the retained parameters in Figs. S1 and S2) resulted in almost all cases in the benchmark calibration (SW-AET-Tr) performing best (Fig. 6). The differences between sun exposed and shade locations were marginal for all calibration targets using AET particularly in terms of simulated dynamics expressed by a correlation coefficient. However, the benchmark calibration also resulted in the greatest uncertainty, with the widest range of parameters and performance scores. Only the AET and Tr calibration targets resulted in less variable performance scores. Surprisingly, the AET and SW-AET calibration targets performed the worst and the Tr and SW-Tr the best. Using only SW data for calibration did not cause model failure in simulating water partitioning, though it decreased performance in comparison with other calibration schemes. The difference for sun exposed and shade locations was also greatest when using only SW data for calibration.

The sensitivity analysis (Table 3) confirmed the expected parameter influence on model performance (KGE). Models calibrated with Tr were most sensitive to the two water partitioning parameters (rE, alpha) together with a soil water content rate parameter (ks2). The SW calibration preferred ks1, Smax and g1 soil water parameters and the AET calibration resulted in one water partitioning parameter (rE) being sensitive together with the soil water parameters ks2 and g1.

# 4.2. Model calibration impact on ecohydrological water partitioning

Analysis of simulated ecohydrological water partitioning for sun

**Table 1**Observed catchment hydroclimatic (wholeplot P, PET, T, RH, and SW at sun and shade locations) summary statistics for the Mejias experimental plot and the period from 2010 to 2013.

	Unit	Mean	SD	Min	Max
Mean annual P	mm	2830	515	2112	3316
Mean annual PET	mm	1599	144	1420	1768
M ean annual T	°C	19.6	0.13	19.5	19.8
Mean RH	%	86.1	1.19	85	87.6
Mean annual SW 0-1m	mm	314;	6.3; 6.2	305;	320;
(shade; sun)		340		331	345
Mean annual SW	mm	734;	21.8;	709;	762;
1-3.5m (shade; sun)		720	6.0	714	725

Table 2
Initial model parameter ranges used in multi-objective calibration and the resulting posterior parameter ranges retaining the best performing 500 parameter sets for water partitioning analysis. The full posterior parameter distributions are further shown in Figs. S1 and S2.

		Initial Parameter Ranges							
Calibration target	rE (-)	alpha (mm)	Smax (mm)	$ks1$ $(h^{-1})$	ks2 (h <sup>-1</sup> )	GW <sub>max</sub> (mm)	g1 (-)	g2 (-)	PF <sub>Scale</sub> (-)
Мах	-0.38	0.2	980	30	15	1470	4.8	5	0.5
Min	-0.1	0.09	610	12	5	1020	3	4	0.3
			Posterior par	ameter distrib	utions with Median	(10th and 90th per	centile)		
SHADE:									
SW-AET-Tr	-0.2 (-0.33; -0.11)	0.09 (0.09; 0.09)	759 (617; 959)	30 (30; 30)	14.8 (6.6; 15)	1358 (1082; 1460)	3.1 (3; 4.8)	4.1 (4; 5)	0.49 (0.27; 0.5
SW	-0.37 (-0.38; -0.19)	0.09 (0.09; 0.1)	695 (610; 764)	30 (30; 30)	5.1 (5; 5.4)	1020 (1020; 1020)	3.7 (3.1; 4.8)	5 (5; 5)	0.33 (0.26; 0.46)
AET	-0.11 (-0.11; -0.10)	0.2 (0.2; 0.2)	610 (610; 610)	30 (30; 30)	12 (10.8; 14.8)	1469 (1468; 1470)	3 (3; 3.1)	5 (5; 5)	0.37 (0.1; 0.5)
Tr	-0.38 (-0.38; -0.32)	0.09 (0.09; 0.09)	980 (980; 980)	30 (30; 30)	11.3 (6.1; 15)	1421 (1307; 1468)	3 (3; 3)	4 (4; 4)	0.5 (0.5; 0.5)
SW-AET	-0.1 (-0.1; -0.1)	0.19 (0.12; 0.2)	793 (622; 931)	30 (30; 30)	15 (9.7; 15)	1465 (1465; 1428)	3.5 (3.1; 4.6)	4 (4; 4)	0.5 (0.27; 0.5)
SW-Tr	-0.22 (-0.38; -0.11)	0.09 (0.09; 0.12)	757 (754; 979)	30 (30; 30)	5 (7.5; 5)	1064 (1023; 1457)	4.8 (3.4; 4.8)	5 (4; 5)	0.49 (0.48; 0.5
SUN:									
SW-AET-Tr	-0.16 (-0.23; -0.11)	0.09 (0.09; 0.19)	910 (630; 972)	30 (30; 30)	14.9 (14.3; 15)	1433 (1152; 1469)	3.1 (3; 4.8)	4.03 (4; 5)	0.5 (0.22; 0.5)
SW	-0.1 (-0.1; -0.1)	0.11 (0.11; 0.11)	980 (944; 980)	30 (30; 30)	15 (15; 15)	1408 (1363; 1469)	3.7 (3.1; 4.6)	5 (5; 5)	0.5 (0.5; 0.5)
AET	-0.1 (-0.11; -0.1)	0.2 (0.2; 0.2)	610 (610; 610)	30 (30; 30)	14.8 (13.4; 15)	1470 (1470; 1470)	3.1 (3; 3.1)	5 (5; 5)	0.43 (0.12; 0.5
Tr	-0.25 (-0.28; -0.23)	0.09 (0.09; 0.09)	980 (980; 980)	30 (30; 30)	15 (15; 15)	1470 (1470; 1470)	3 (3; 3)	4 (4; 4)	0.5 (0.5; 0.5)
SW-AET	-0.1 (-0.1; -0.1)	0.2 (0.09; 0.2)	926 (614; 980)	30 (30; 30)	15 (15; 15)	1467 (1034; 1470)	3.5 (3.1; 4.6)	4 (4; 5)	0.5 (0.3; 0.5)
SW-Tr	-0.25 (-0.28; -0.11)	0.09 (0.09; 0.09)	980 (911; 980)	30 (30; 30)	15 (15; 15)	1467 (1031; 1470)	4.1 (3.1; 4.8)	4 (4; 4)	0.5 (0.5; 0.5)

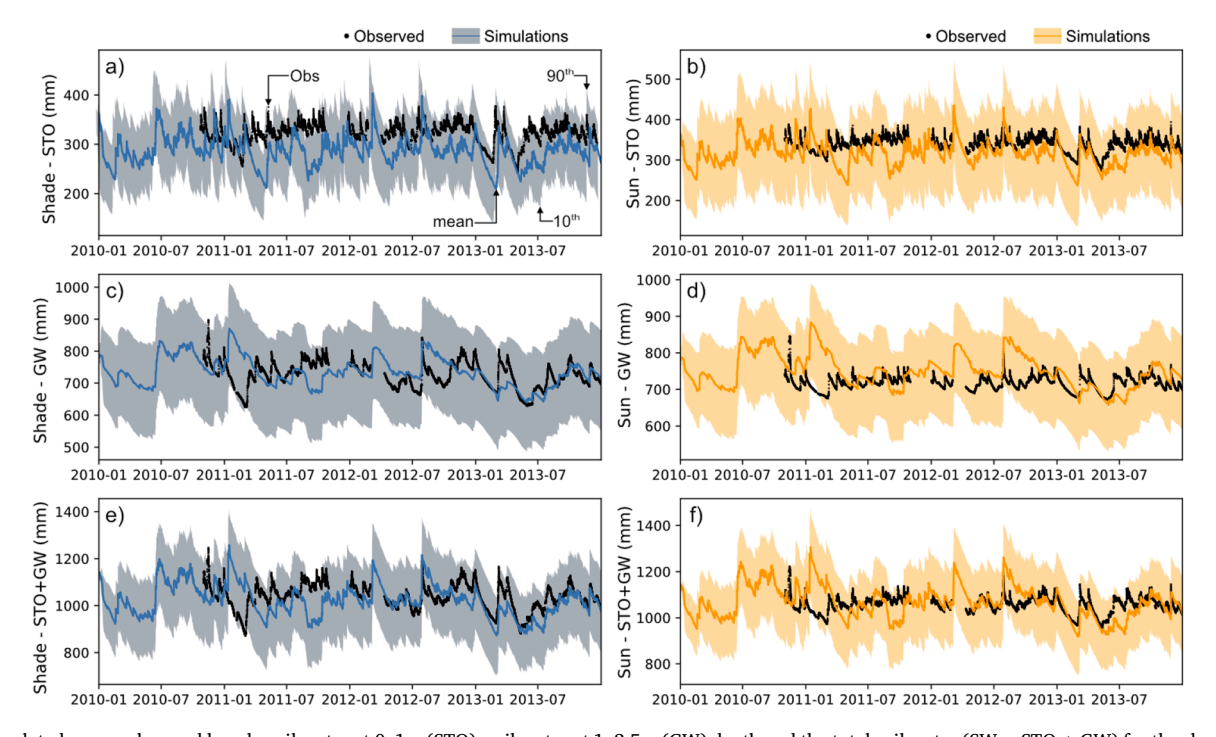


Fig. 4. Simulated versus observed hourly soil water at 0-1m (STO), soil water at 1-3.5m (GW) depth and the total soil water (SW = STO + GW) for the shade and sun exposed locations using the benchmark calibration target SW-AET-Tr obtained from the 500 highest scoring (best) simulations.

exposed and shade locations was based on ternary plots of the Ei, Es and total Tr flux components as percentage contributions to total AET according to the different calibration targets (Fig. 7). Unsurprisingly, only the Tr calibration resulted in a constrained set of >70% transpiration

estimates of total AET, closest to the measured Tr/AET ratio of 0.91 for the shade and 0.73 for the sun exposed location. The absolute numbers and water partitioning statistics can be found in Table 4. In contrast, the AET and SW-AET calibration targets consistently resulted in much lower

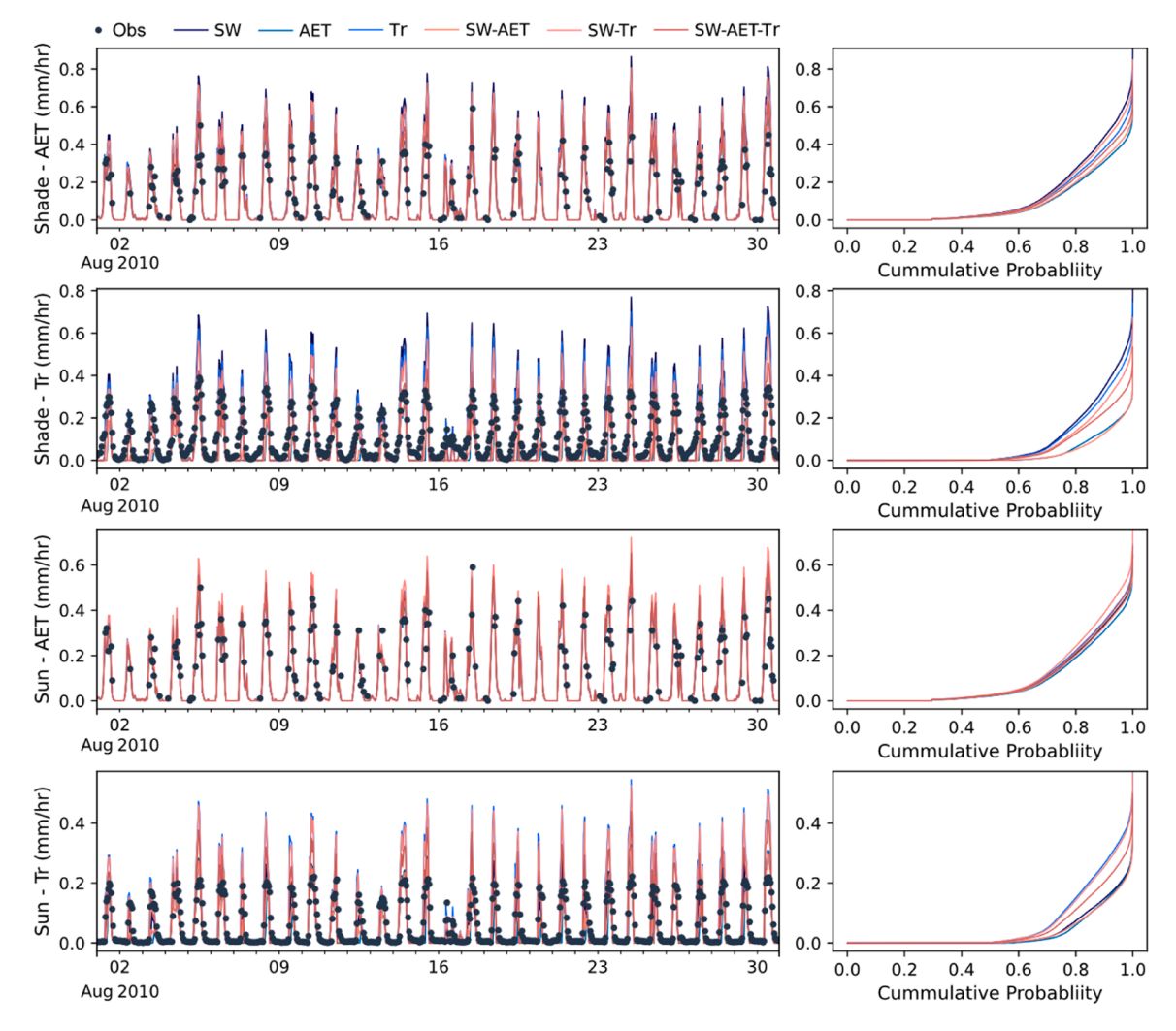


Fig. 5. Hourly observed and simulated AET and Tr during August 2010 for shade and sun, and the corresponding cumulative probability distributions of simulations for the complete period from 2010 to 2013. The colour lines indicate the different calibration targets. Note that the Tr rates are scaled to the sun exposed and shade locations whereas the AET flux represents the whole plot.

Tr/AET ratios of around 0.5. Including SW as a calibration target resulted in reasonable water partitioning simulations, but with a much wider range of Tr/AET ratios and more difficulty to identify the best solutions. Despite the best performance of the benchmark calibration, simulation of water partitioning resulted more uncertain and led us to reject our initial working hypothesis.

Similarly, we separated out the simulated soil water losses as the total evaporation (Ei + Es), Tr and groundwater recharge flow Gr (aquifer recharge) in Fig. 8. Despite differently simulated Tr/AET fractions, the simulated fraction of Gr remained largely indifferent amongst calibration targets. Results suggested that Gr corresponds to 60–75% of the total soil water losses, and Tr corresponds to 10 – 30%, except for the results obtained with AET and SW-AET model calibrations, where Tr is  $\sim\!10\%$  of the soil water losses.

Additionally to Fig. 5, we arbitrarily selected a 24-hour period to show how the model simulated the diurnal variability with different calibration targets (Fig. 9) and calculated performance metrics (Table 5) for the median Tr simulation from the 500 retained best parameter sets of a calibration (2010) and validation period (2011). Simulations that involved transpiration as a target generally reproduced the diurnal variability with a good performance of KGE>0.6, CC>0.8 and RMSE<0.08 for both the sun and shade plots. The validation period resulted in better performance considering all metrics compared to the calibration and slightly better performance for the sun plot compared to

the shade. Again, including transpiration as a calibration target improved the simulations (Fig. 9), which was also reflected in a large difference of performance (lowest performance for AET with KGE<0.3). The models reproduced the onset of daytime transpiration but failed to simulate small night-time transpiration fluxes measured for shaded coffee (Fig. 9).

# 5. Discussion

# 5.1. Can a simple model be used to reasonably partition ecohydrological fluxes?

The EcoHydroPlot model could be considered as a relatively parsimonious way of modelling water fluxes between the soil and the atmosphere as mediated by vegetation, even with nine calibrated parameters (Collenteur et al., 2021). Reducing the number of calibrated parameters could further be achieved by linearizing one or more of the power-function type flux equations Eq. (7) and (9). However, soil and groundwater fluxes are usually best modelled with non-linear transfer functions as shown by Fenicia et al., (2006) since groundwater related vertical and lateral fluxes are intermittent pulses rather than constant flux rates. The latter was shown for the tropics in general (Jasechko et al., 2014) and Costa Rica specifically based on stable isotope data (Sanchez-Murillo and Birkel, 2016). Consequently, the calibrated

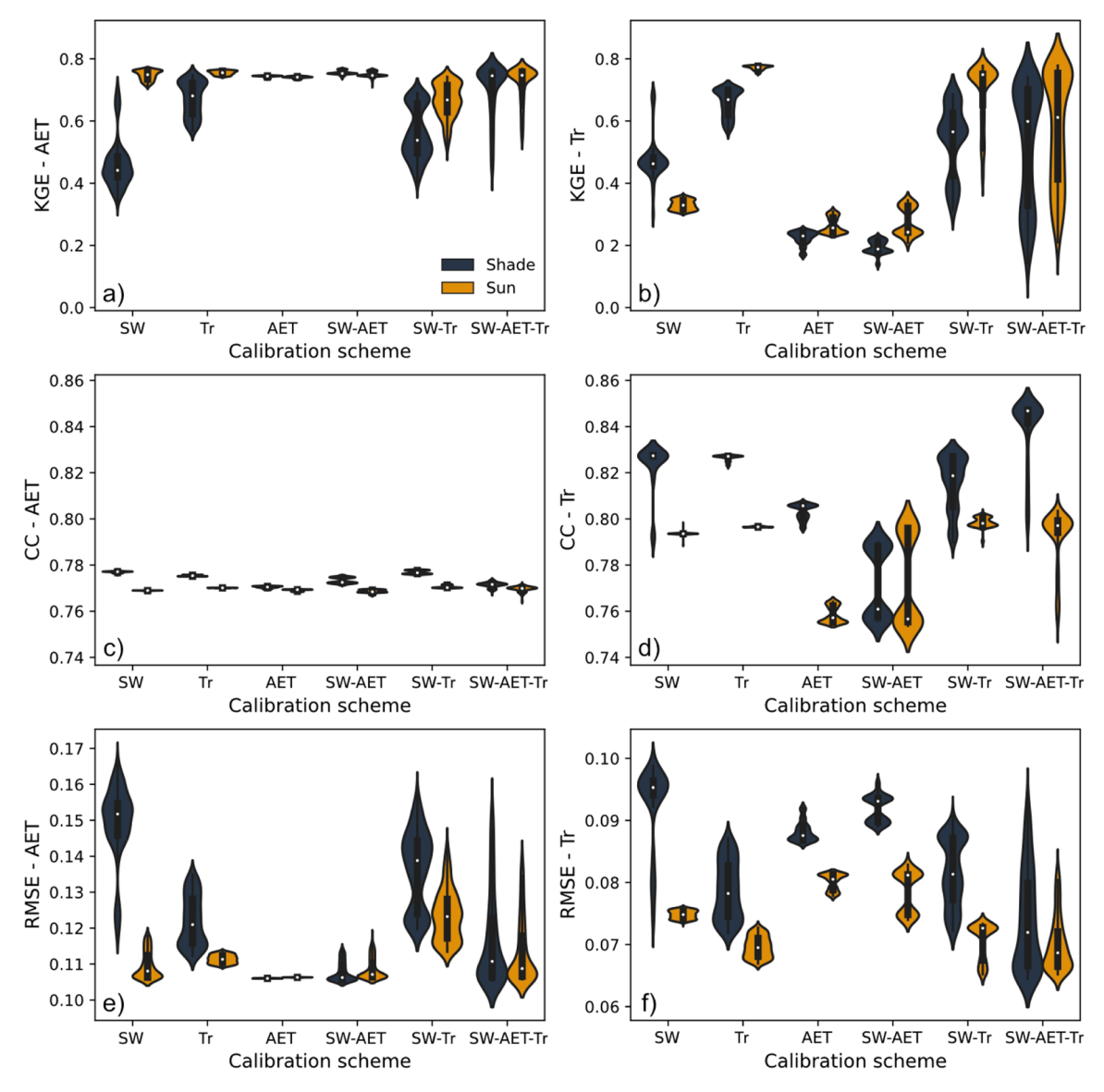


Fig. 6. Violin plots of model performance metrics (KGE, CC, RMSE) for measured vs. simulated actual evapotranspiration (AET) (a, c, e) and transpiration (Tr) (b, d, f) shade (blue) and sun exposed (yellow) plots using all calibration targets (SW, T, SW-AET, SW-Tr, and benchmark SW-AET-Tr).

**Table 3**Parameter sensitivity ranking using LH—OAT for the KGE performance metric of the calibration targets SW (shade), wholeplot AET and Tr (shade) only. The first three most sensitive parameters are displayed in bold and italics.

Parameter	Rank (SW)	Rank (AET)	Rank (Tr)
rE	0.083	0.49	0.59
alpha	0.076	0.045	0.33
ks1	0.11	0.1	0.012
ks2	0	0.116	0.025
Smax	0.34	0.008	0.0029
g1	0.32	0.158	0.02
g2	0	0.06	0.014
GWmax	0	0.002	0.003
PFscale	0.064	0.018	0.002

power-function parameters g1 and g2 resulted in highly non-linear values always > 3 independent of the calibration target (Table 3 and Figs. S1 and S2). The non-linear relationship of soil storage and soil fluxes in simple spatially-aggregated models was also emphasized by Maneta et al. (2018). Furthermore, tropical high rainfall areas often result in larger plant-available soil water storages (if soil characteristics

allow) compared to temperate regions (Gao et al., 2014). In the Mejias study plot, average soil moisture storage was measured at over 1000mm (Table 1) with roots observed to a depth of 3.5m (Defrenet et al., 2016). Even though root density is highest in the first metre of soil, such a relatively deep root profile is clearly influenced by the presence of the *Erythrina* shade trees modulating plant transpiration, which we tried to emulate with the model structure (Fig. 3). The presence of deeper roots also helps maintain high hydraulic conductivities and infiltrability (Benegas et al., 2014) due to macropores and soil pipes, a widespread phenomenon across the tropics as described by Chappell (2010). Therefore, preferential flow paths are non-linear in their response and should not be linearly parameterized within a model.

Additionally, to the soil water fluxes, the ecohydrological water partitioning was based on a simplified interception module using LAI as the main indicator (Fig. 2) to discriminate amongst vegetation types and intra-annual vegetation dynamics. The model uses an interpolated continuous LAI time series input function based on weekly measurements as a surrogate for interception storage capacity. At higher LAI, more water can be efficiently intercepted by the vegetation and is subjected to canopy interception evaporation and throughfall similar to, for example, van Dijk and Bruijnzeel (2001). The interception routine here

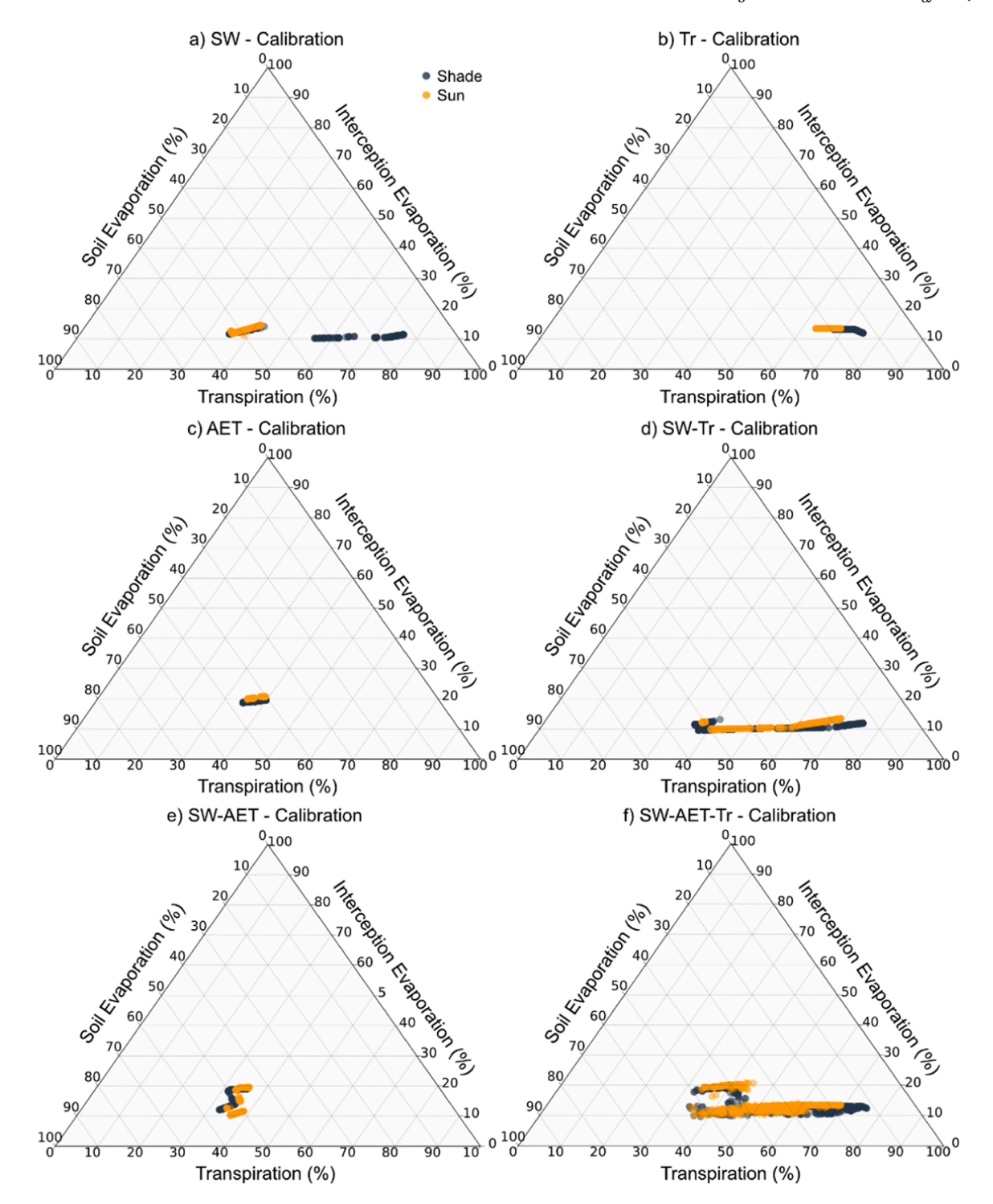


Fig. 7. Ecohydrological flux mapping of partitioned green (transpiration) and blue (soil and interception evaporation) water using the retained best 500 simulations after calibration.

uses only two calibrated parameters and does not need further storage capacity or threshold parameters compared to, for example, the more complex Rutter interception model (Rutter et al., 1971) and others (Muzylo et al., 2009). Interestingly, all 15 reviewed interception models by Muzylo et al. (2009) used a formulation of Penman-Monteith to dimension PET. The utility of LAI as an indicator of ecohydrological water partitioning in the tropics was demonstrated by Taugourdeau et al. (2014), who showed that LAI is a direct indicator of coffee yield at the Mejias site, which was indirectly related to higher transpirations rates of shaded coffee and resulting higher productivity. For another

example, Benyon and Doody (2004) showed a positive relationship of measured LAI with measured Tr rates in reforestation plots in tropical Australia. Large-scale AET assessments that documented a vegetation greening and an increasing AET trend over past decades also relied on LAI (Pascolini-Campbell et al., 2021), but Zhang et al. (2021) showed that LAI does not reflect any physiological negative feedbacks such as stomatal closure due to increased CO<sub>2</sub>. Nonetheless, such limitations need careful consideration at larger and long-term scales, but maybe less so for site-specific studies as studied here with an emphasis on model parsimony.

Table 4
Summary of the mean annual water balance and simulated water partitioning metrics (P, AET, Tr/AET, Tr/P) derived from the 500 best simulations after calibration with different targets. \*Metrics only used available data for observed (obs) vs. simulated omitting any incomplete pairs from gaps in AET and Tr measurements.

Plot	Target	Variable	Mean	SD	25th	50th	75th
	Obs	P*	2264	1342	2112	2858	3032
Wholeplot	Obs	AET	869	71	818	859	910
Shade	Obs	Tr-AET	0.91	0.04	0.90	0.91	0.92
Shade	SW	Tr-AET	0.69	0.07	0.32	0.69	0.77
Shade	T	Tr-AET	0.72	0.06	0.64	0.72	0.76
Shade	AET	Tr-AET	0.38	0.00	0.34	0.38	0.39
Shade	SW-AET	Tr-AET	0.33	0.06	0.29	0.33	0.37
Shade	SW-T	Tr-AET	0.57	0.08	0.32	0.57	0.76
Shade	SW-AET-T	Tr-AET	0.55	0.02	0.32	0.55	0.76
Sun	Obs	Tr-AET	0.73	0.17	0.67	0.73	0.79
Sun	SW	Tr-AET	0.37	0.01	0.33	0.37	0.40
Sun	T	Tr-AET	0.66	0.01	0.62	0.66	0.69
Sun	AET	Tr-AET	0.36	0.00	0.34	0.36	0.38
Sun	SW-AET	Tr-AET	0.35	0.01	0.31	0.35	0.38
Sun	SW-T	Tr-AET	0.58	0.01	0.35	0.58	0.69
Sun	SW-AET-T	Tr-AET	0.50	0.01	0.32	0.50	0.69
Shade	Obs	Tr-P	0.27	0.04	0.26	0.27	0.29
Shade	SW	Tr-P	0.27	0.01	0.11	0.27	0.30
Shade	T	Tr-P	0.24	0.01	0.21	0.24	0.27
Shade	AET	Tr-P	0.10	0.02	0.09	0.10	0.11
Shade	SW-AET	Tr-P	0.09	0.00	0.08	0.09	0.10
Shade	SW-T	Tr-P	0.21	0.01	0.11	0.21	0.28
Shade	SW-AET-T	Tr-P	0.18	0.03	0.08	0.18	0.30
Sun	Obs	Tr-P	0.20	0.07	0.17	0.20	0.22
Sun	SW	Tr-P	0.10	0.01	0.09	0.10	0.11
Sun	T	Tr-P	0.19	0.02	0.17	0.19	0.21
Sun	AET	Tr-P	0.09	0.01	0.08	0.09	0.10
Sun	SW-AET	Tr-P	0.09	0.01	0.08	0.09	0.10
Sun	SW-T	Tr-P	0.18	0.02	0.10	0.18	0.21
Sun	SW-AET-T	Tr-P	0.14	0.02	0.08	0.14	0.21

# 5.2. Which calibration targets provide the most information content?

Our multi-objective calibration approach to assess the influence of different calibration targets goes back to Madsen (2000) and follows the idea of Crow et al., (2003) who used streamflow and radiometric temperature data to improve predictions of AET simulated by a land surface model. Much has happened since and here, the SW measurements provided basic and necessary hydrological background data for model calibration with reasonable model performance for all calibration targets of KGE > 0.6 (Fig. 4). Additionally, to SW as a calibration target, measured AET provided useful data to close the water balance (Fig. 5) but did not significantly influence ecohydrological water partitioning within the model (Table 4) and performed poorly simulating transpiration (Fig. 9, Table 5). The benefits of using AET data for model calibration was recently shown by Arciniega et al. (2022) for Costa Rica. However, their large-scale modelling used satellite ET estimates, which would not necessarily provide information at the desired smaller plot scale resulting in additional uncertainty (Franks et al., 1997). Therefore, using measured AET and Tr data for hydrological model calibration is still rather rare (except for Schreiner-McGraw et al. (2022) who used a much more complex Community Land Surface model), mainly due to the difficulty to upscale Tr from individual plants or stands to plot and catchment scales (Ford et al., 2007; Aparecido et al., 2016). At the Mejias plot, the sap-flux derived Tr measurements have also been validated by Eddy-Covariance measurements and deemed reasonable by

Both the measured Tr data alone, and in combination with SW, as calibration targets resulted in the most robust ecohydrological water partitioning estimates (Figs. 7 and 8). The simple conceptual EcoHydroPlot model was able to provide reasonable water flux and balance estimates for the humid tropical test plot at an hourly scale. If calibrated using data on Tr, the simulations also matched observed Tr/AET ratios

of between 0.7 and 0.9 and Tr/P of 0.2 for the sun exposed and Tr/ P=0.27 for the shade locations (Table 4). In a cross-check comparison, such Tr/AET values were found for the study site using an isotope-based mass balance approach by Iraheta et al. (2021). Gomez-Delgado et al. (2011) showed relatively similar water partitioning ratios (Tr/P=0.2) for the Mejias catchment scale modelled for 2010. Their groundwater recharge estimates of Gr/P=0.67 also matched our findings of Gr/P=0.6 to 0.75. Vezy et al., (2018) simulated a total AET of 870mm/yr for 2011 closely matching observed values and our estimates with a physically-based, and much more complex energy balance model (MAESPA). Despite simulating a similar Tr/P=0.28, their Tr/AET of 0.46 resulted lower with a relatively high total evaporation (Ei + Es) to AET ratio of 0.54 compared to our simulations. The EcoHydroPlot simulations for the shade plot were generally better (except for simulated transpiration due to night-time transpiration fluxes the model is unable to reproduce, Fig. 9) and even resulted in a reasonable Tr/AET ratio on one occasion with only SW as calibration target. However, the latter could not be reproduced for the sun exposed plot and might therefore be considered an outlier (Fig. 6). Based on our calibration results and rejection of the benchmark calibration including all targets, future monitoring efforts for similar research questions should prioritize inclusion of direct Tr measurements in form of sap flux and/or Eddy Covariance to enhance simulated ecohydrological water partitioning.

#### 5.3. Water use in tropical coffee plantations

Early work on coffee transpiration in the tropics by Gutiérrez and Meinzer (1994) showed a tight regulation of wind and stomata dynamics to environmental variables. In southern Costa Rica, van Kanten and Vaast (2006) found increased Tr for shaded Arabica coffee compared to sun exposed coffee similar to our modelling and available measurements. The latter higher shade Tr rates compared to sun exposed locations presumably reflect greater sapflow in shade trees and the suppression of Es by shading. Higher Tr was found to increase coffee productivity at the Mejias site by Taugourdeau et al. (2014) and Chinchilla-Soto et al. (2021) who found greater shade coffee water use efficiencies at a coffee plantation in Central Costa Rica. Shaded coffee enhanced bean quality as found by Vaast et al. (2006). Even though not specifically tested, and a likely result of minor differences in LAI between sun and shade location, we did not find increased groundwater losses or any significant hydrological differences (Fig. 8). Despite slightly lower upper soil storage at the shaded plot due to increased Tr compared to the sun exposed location, the high storage capacity of the soils can well compensate this vegetation influence of a generally energy-limited rather than water-limited environment.

Coffee shading altogether could provide a successful measure against the concerns over climate change impacted reduced coffee productivity (Pham et al., 2019), since shading suppresses E and enhances water use efficiency at the study site. Our model could be used and transferred to other sites for impact assessments of a combined land cover and climate change.

# 6. Conclusions and outlook

We developed and tested the relatively parsimonious conceptual ecohydrology EcoHydroPlot model with detailed data from the Mejias Coffee-Flux agroforestry experimental site in humid tropical Costa Rica. Measured SW, AET and Tr were used as calibration targets in a multi-objective optimization calibration exercise – making use of this unique data set of ecohydrological flux measurements under different land uses in the tropics - to assess their influence on ecohydrological water partitioning of simulated vs. observed water losses to the atmosphere (Ei, Es, Tr) and to the aquifer (Gr). Such combination of (i) measurements of ecohydrological fluxes under different, typical land uses in the tropics; (ii) use of these data within a multi-calibration modelling framework in a (iii) conceptual model for wider applicability to inform stakeholders is

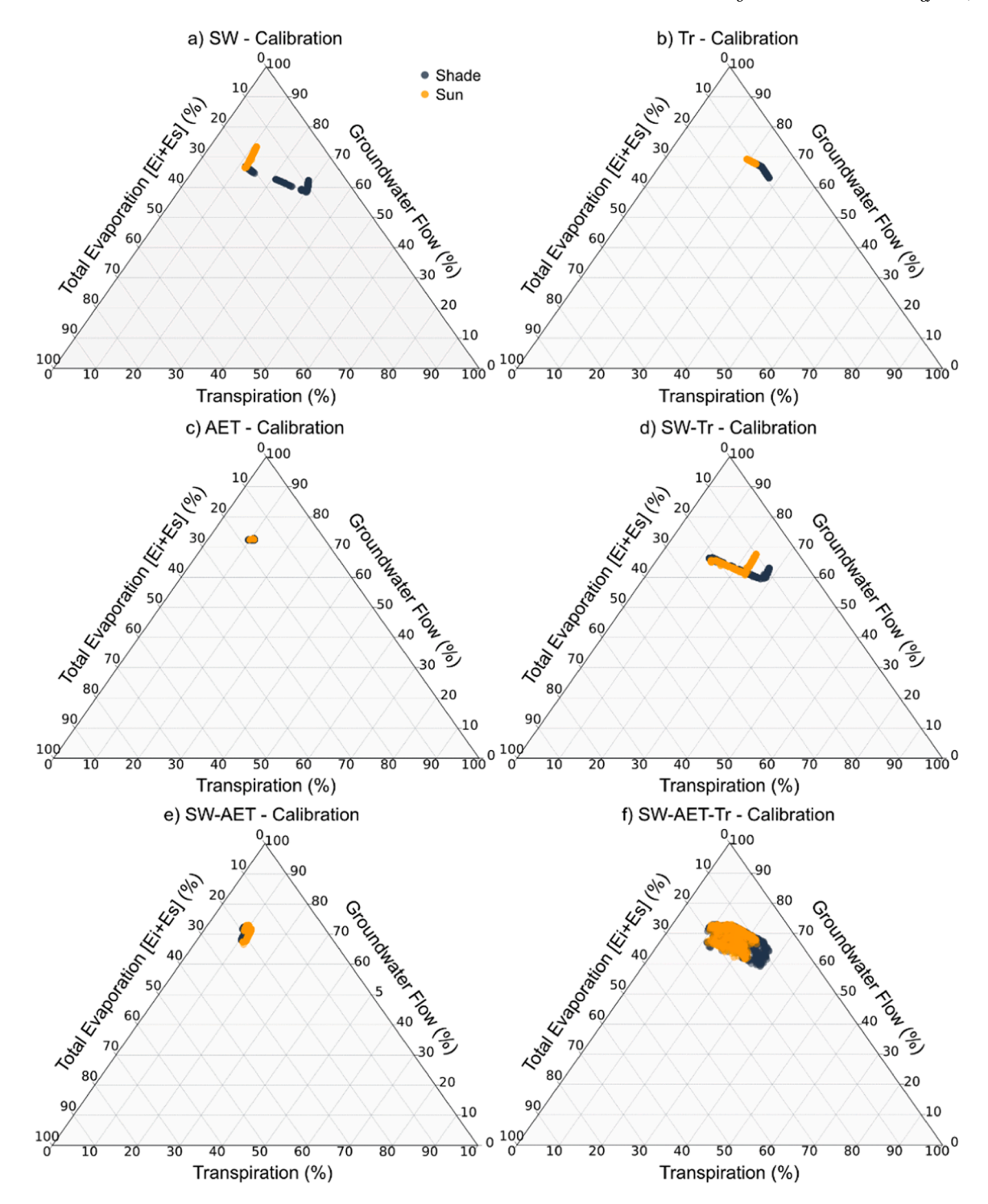


Fig. 8. Ecohydrological flux mapping of total water losses of partitioned green (transpiration) and blue (total evaporation as the sum of soil and interception evaporation plus groundwater recharge Gr) water using the retained best 500 simulations after calibration.

– to our knowledge – a novel way forward to bridge the gap towards a science-based decision making. The consistency in water partitioning was assessed using a flux mapping approach that visualizes how different calibration targets pull the model towards green or blue water-dominated fluxes. The main outcome was that only including Tr as a calibration target resulted in matching Tr/AET ratios for sun exposed and shaded coffee locations with other targets such as SW pulling the model mostly towards simulating evaporation fluxes. We therefore rejected our initial hypothesis that including as many calibration targets as possible improves model representation of ecohydrological water

partitioning. These findings emphasize the value of measured green water fluxes (such as Tr) for model calibration improving on simulated transpiration and water partitioning, which should be a key measurement included in all ecohydrology monitoring and modelling studies. Our simple model provides a useful and parsimonious tool to assess land cover change and its impact on green and blue water fluxes, which of course is not only applicable in tropical environments.

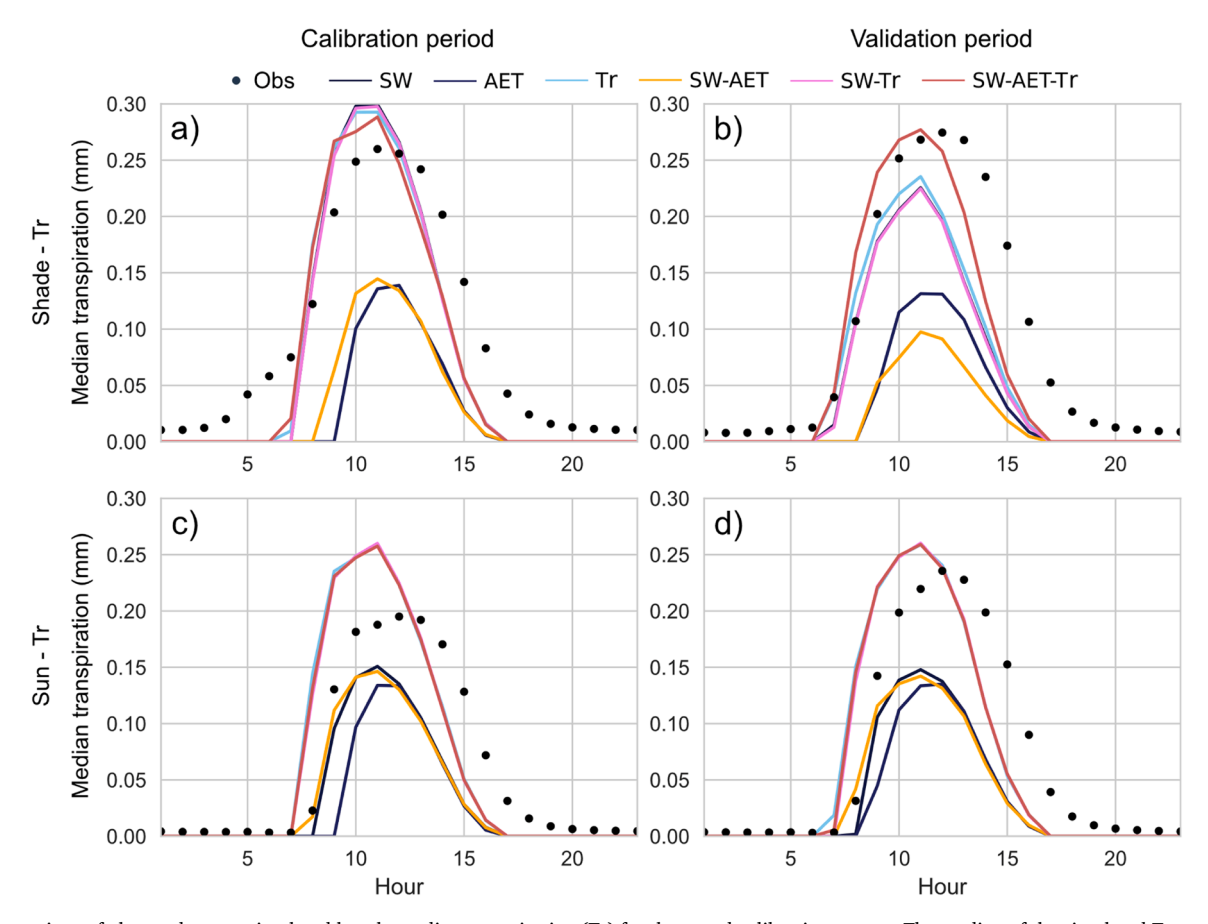


Fig. 9. Comparison of observed versus simulated hourly median transpiration (Tr) for the tested calibration targets. The median of the simulated Tr was calculated from the best-performing 500 parameter sets after calibration and illustrated for an arbitrarily selected 24 hour calibration (2010) and validation (2011) period.

Table 5
Performance metrics (KGE, CC, RMSE) of the median hourly transpiration simulation using different calibration targets. The calibration and validation periods correspond to 2010 and 2011, respectively. The median simulation was derived from the retained 500 best-performing parameter sets after calibration (Table 2).

		Shade		Sun			
Period	Calibration target	KGE	CC	RMSE	KGE	CC	RMSE
Calibration	SW	0.59	0.86	0.075	0.53	0.81	0.052
	Tr	0.62	0.86	0.072	0.56	0.81	0.066
	AET	0.27	0.81	0.082	0.47	0.77	0.057
	SW-AET	0.33	0.83	0.077	0.53	0.81	0.052
	SW-Tr	0.59	0.86	0.075	0.56	0.82	0.066
	SW-AET-Tr	0.69	0.86	0.065	0.56	0.82	0.066
Validation	SW	0.64	0.80	0.076	0.25	0.82	0.091
	Tr	0.68	0.80	0.075	0.71	0.83	0.072
	AET	0.23	0.81	0.091	0.21	0.80	0.095
	SW-AET	0.11	0.77	0.101	0.24	0.82	0.092
	SW-Tr	0.63	0.80	0.076	0.72	0.83	0.071
	SW-AET-Tr	0.77	0.84	0.069	0.71	0.83	0.071

#### CRediT authorship contribution statement

Christian Birkel: Conceptualization, Methodology, Data curation, Writing – original draft, Visualization, Investigation, Supervision, Writing – review & editing. Saul Arciniega-Esparza: Conceptualization, Methodology, Data curation, Writing – original draft, Visualization, Investigation, Writing – review & editing. Marco P. Maneta: Conceptualization, Writing – review & editing. Jan Boll: Conceptualization, Writing – review & editing. Jamie Lee Stevenson:

Conceptualization, Visualization, Investigation, Writing – review & editing. Laura Benegas-Negri: Conceptualization, Data curation, Writing – original draft, Writing – review & editing. Dörthe Tetzlaff: Conceptualization, Writing – review & editing. Chris Soulsby: Conceptualization, Methodology, Data curation, Writing – original draft, Supervision, Funding acquisition, Writing – review & editing.

### **Declaration of Competing Interest**

The authors declare the following financial interests/personal relationships which may be considered as potential competing interests: Chris Soulsby reports financial support was provided by Leverhulme Trust.

#### Data availability

Data will be made available on request.

#### Acknowledgments

This study was funded by the Leverhulme Trust ISOLAND project (RPG-2018–375) and we thank Dr. Aaron Neill for his contributions to data preparation and discussions on the modelling approach. We also acknowledge the Coffee-Flux study and particularly Dr. Olivier Roupsard for such a rich data source made available to the scientific community.

#### Supplementary materials

Supplementary material associated with this article can be found, in the online version, at doi:10.1016/j.agrformet.2023.109870.

#### References

- Aparecido, L.M.T., Miller, G.R., Cahill, A.T., Moore, G.W., 2016. Comparison of tree transpiration under wet and dry canopy conditions in a Costa Rican premontane tropical forest. Hydrol. Process. 30 (26), 5000–5011. https://doi.org/10.1002/ hvp.10960.
- Arciniega-Esparza, S., Birkel, C., Chavarría-Palma, A., Arheimer, B., Breña-Naranjo, J.A., 2022. Remote sensing-aided rainfall-runoff modeling in the tropics of Costa Rica. Hydrol. Earth Syst. Sci. 26 (4), 975–999. https://doi.org/10.5194/hess-26-975-2022.
- Allen R., Pereira L., Raes D., Smith M., 1998. Crop evapotranspiration. Guidelines for computing crop water requirements. FAO Irrigation and Drainage Paper 56, p. 301. Available at http://www.fao.org/docrep/X0490E/X0490E00.htm.
- Baldocchi, D., et al., 2001. FLUXNET: a new tool to study the temporal and spatial variability of ecosystem-scale carbon dioxide, water vapor, and energy flux densities. Bull. Am. Meteorol. Soc. 82, 2415–2434.
- Benegas, L., Ilstedt, U., Roupsard, O., Jones, J., Malmer, A., 2014. Effects of trees on infiltrability and preferential flow in two contrasting agroecosystems in Central America. Agric. Ecosyst. Environ. 183, 185–196.
- Benyon, R.G., Doody, T.M., 2004. Water Use by Tree Plantations in South East South Australia. CSIRO Forestry and Forest Products, Mt Gambier.
- Birkel, C., Soulsby, C., Tetzlaff, D., 2012. Modelling the impacts of land cover change and payment for ecosystems services schemes on stream flow dynamics of a tropical forest headwater catchment. Hydrol. Sci. J. https://doi.org/10.1080/02626667.2012.728707.
- Charbonnier, F., le Maire, G., Dreyer, E., Casanoves, F., Christina, M., Dauzat, J., Eitel, J. U.H., Vaast, P., Vierling, L.A., Roupsard, O., 2013. Competition for light in heterogeneous canopies: application of MAESTRA to a coffee (coffea Arabica L.) agroforestry system. Agric. For. Meteorol. 181, 152–169.
- Chappell, N.A., 2010. Soil pipe distribution and hydrological functioning within the humid tropics: a synthesis. Hydrol. Proces. 24 (12), 1567–1581.
- Chinchilla-Soto, C., Durán-Quesada, A.M., Monge-Muñoz, M., Gutiérrez-Soto, M.V., 2021. Quantifying the annual cycle of water use efficiency, energy and CO2 fluxes using micrometeorological and physiological techniques for a coffee field in Costa Rica. Forests 12, 889. https://doi.org/10.3390/f12070889.
- Collenteur, R.A., Bakker, M., Klammler, G., Birk, S., 2021. Estimation of groundwater recharge from groundwater levels using nonlinear transfer function noise models and comparison to lysimeter data. Hydrol. Earth Syst. Sci. 25 (5), 2931–2949. https://doi.org/10.5194/hess-25-2931-2021.
- Crow, W.T., Wood, E.F., Pan, M., 2003. Multiobjective calibration of land surface model evapotranspiration predictions using streamflow observations and spaceborne surface radiometric temperature retrievals. J. Geophys. Res. 108 (D23), 4725. https://doi.org/10.1029/2002JD003292.
- Deb, K., Pratap, A., Agarwal, S., Meyarivan, T., 2002. A fast elitist non-dominated sorting genetic algorithm: NSGA-II. IEEE Trans. Evol. Comput. 6 (2), 182–197.
- Defrenet, E., Roupsard, O., Van den Meersche, K., Charbonnier, F., Perez-Molina, J.P., Khac, E., Prieto, I., Stokes, A., Roumet, C., Rapidel, B., et al., 2016. Root biomass, turnover and net primary productivity of a coffee agroforestry system in costa rica: effects of soil depth, shade trees, distance to row and coffee age. Ann. Bot. 118, 833–851.
- Douinot, A., Tetzlaff, D., Maneta, M., Kuppel, S., Soulsby, C., 2019. Ecohydrological modelling with EcH<sub>2</sub>O-iso to quantify forest and grassland effects on water partitioning and flux ages. Hydrol. Proces. https://doi.org/10.1002/hyp.13480.
- Fenicia, F., Savenije, H.H.G., Margen, P., Pfister, L., 2006. Is the groundwater reservoir linear? Learning from data in hydrological modelling. Hydrol. Earth Syst. Sci. 10, 139–150. https://doi.org/10.5194/hess-10-139-2006.
- Ford, C.R., Hubbard, R.M., Kloeppel, B.D., Vose, J.M., 2007. A comparison of sap flux-based evapotranspiration estimates with catchment-scale water balance. Agricul. For. Meteorol. 145, 176–185.
- Franks, S., Beven, K., Quinn, P., Wright, I., 1997. On the sensitivity of soil-vegetation-atmosphere transfer (SVAT) schemes: equifinality and the problem of robust calibration. Agricul. For. Meteorol. 86, 63–75.
- Gao, H., Hrachowitz, M., Schymanski, S.J., Fenicia, F., Sriwongsitanon, N., Savenije, H. H.G., 2014. Climate controls how ecosystems size the root zone storage capacity at catchment scale. Geophys. Res. Lett. 41, 7916–7923. https://doi.org/10.1002/ 2014.061668
- Gómez-Delgado, F., Roupsard, O., le Maire, G., Taugourdeau, S., Perez, A., van Oijen, M., Vaast, P., Rapidel, B., Harmand, J.M., Voltz, M., Bonnefond, J.M., Imbach, P., Moussa, R., 2011. Modelling the hydrological behaviour of a coffee agroforestry basin in Costa Rica. Hydrol. Earth Syst. Sci. 15, 369–392.
- Granier, A., Biron, P., Breda, N., Pontailler, J.Y., Saugier, B., 1996. Transpiration of trees and forest stands: short and longterm monitoring using sapflow methods. Glob. Chan. Biol. 2 (3), 265–274.
- Grip, H., Fritsch, J.M., Bruijnzeel, L.A., 2005. Soil and water impacts during forest conversion and stabilisation to new land use. In: Bonell M, Bruijnzeel LAJ (eds). Forest, Water and People in the Humid Tropics. Cambridge University Press, New York, pp. 561–589. https://doi.org/10.1017/CBO9780511535666.029.
- Griscom, B.W., et al., 2017. Natural climate solutions. Proc. Natl. Acad. Sci. U. S. A. 114, 11645–11650.

- Gutiérrez, M.V., Meinzer, F.C., 1994. Regulation of transpiration in coffee hedgerows: covariation of environmental variables and apparent responses of stomata to wind and humidity. Plant Cell Environ. 17, 1305–1313.
- Harmand, J.M., Avila, H., Dambrine, E., Skiba, U., de Miguel, S., Renderos, R.V., Oliver, R., Jimenez, F., Beer, J., 2007. Nitrogen dynamics and soil nitrate retention in a Coffea arabica Eucalyptus deglupta agroforestry system in Southern Costa Rica. Biogeochem 85, 125–139.
- Jasechko, S., Sharp, Z.D., Gibson, J.J., Birks, S.J., Yi, Y., Fawcett, P.J., 2013. Terrestrial water fluxes dominated by transpiration. Nature 496, 347–350. https://doi.org/ 10.1038/nature11983.
- Kath, J., Byrareddy, V.M., Craparo, A., Nguyen-Huy, T., Mushtaq, S., Cao, L., Bossolasco, L., 2020. Not so Robust: Robusta coffee production is highly sensitive to temperature. Glob. Chang. Biol. 26, 3677–3688.
- Khatami, S., Peel, M.C., Peterson, T.J., Western, A.W., 2019. Equifinality and flux mapping: a new approach to model evaluation and process representation under uncertainty. Wat. Resour. Res. 55, 8922–8941. https://doi.org/10.1029/ 2018WR023750.
- Kling, H., Fuchs, M., Paulin, M., 2012. Runoff conditions in the upper Danube basin under an ensemble of climate change scenarios. J. Hydrol. 424, 264–277. https:// doi.org/10.1016/j.jhydrol.2012.01.011.
- Kuppel, S., Tetzlaff, D., Maneta, M.P., Soulsby, C., 2018. EcH2O-iso 1.0: water isotopes and age tracking in a process-based, distributed ecohydrological model. Geosci. Model Dev. 11, 3045–3069. https://doi.org/10.5194/gmd-11-3045-2018.
- Leuning, R., Kelliher, F., Pury, D.d., Schulze, E.D., 1995. Leaf nitrogen, photosynthesis, conductance and transpiration: scaling from leaves to canopies. Plant Cell Environ. 18 (10), 1183–1200.
- LI-COR, 1992. LAI-2000 Plant Canopy Analyser: Instruction Manual. LI-COR Inc., Lincoln, NE.
- Madsen, H., 2000. Automatic calibration of a conceptual rainfall-runoff model using multiple objectives. J. Hydrol. 235, 276–288.
- Maneta, M.P., Silverman, N.L., 2013. A spatially distributed model to simulate water, energy, and vegetation dynamics using information from regional climate models. Earth Interact. 17 (11) https://doi.org/10.1175/2012EI000472.1.
- Maneta, M., Soulsby, C., Kuppel, S., Tetzlaff, D., 2018. Conceptualizing catchment storage dynamics and nonlinearities. Hydrol. Process. 32, 3299–3303.
- Meli, P., Holl, K.D., Rey Benayas, J.M., Jones, H.P., Jones, P.C., Montoya, D., Mateos, D. M., 2017. A global review of past land use, climate, and active vs. passive restoration effects on forest recovery. PLOS One 12 (2), e0171368. https://doi.org/10.1371/journal.pone.0171368.
- Muzylo, A., Llorens, P., Valente, F., Keizer, J., Domingo, F., Gash, J., 2009. A review of rainfall interception modelling. J. Hydrol. 370 (1–4), 191–206. https://doi.org/ 10.1016/j.jhydrol.2009.02.058.
- Ovalle-Rivera, O., Läderach, P., Bunn, C., Obersteiner, M., Schroth, G., 2015. Projected shifts in coffea arabica suitability among major global producing regions due to climate change. PLOS One 10, e0124155.
- Pascolini-Campbell, M., Reager, J.T., Chandanpurkar, H.A., Rodell, M., 2021. A 10% increase in global land evapotranspiration from 2003 to 2019. Nature 593, 543–547.
- Pham, Y., Reardon-Smith, K., Mushtaq, S., Cockfield, G., 2019. The impact of climate change and variability on coffee production: a systematic review. Clim. Chang. 156, 609–630.
- Philpott, S.M., Arendt, W.J., Armbrecht, I., Bichier, P., Diestch, T.V., Gordon, C., Greenberg, R., Perfecto, I., Reynoso-Santos, R., Soto-Pinto, L., Tejeda-Cruz, C., Williams-Linera, G., Valenzuela, J., Zolotoff, J.M., 2008. Biodiversity loss in latin american coffee landscapes: review of the evidence on ants, birds, and trees. Conserv. Biolog. 22, 1093–1105.
- R Core Team, 2022. R: A Language and Environment For Statistical Computing. R Foundation for Statistical Computing, Vienna, Austria. Available from. https://www. R-project.org/.
- Roupsard, O., Bonnefond, J.M., Irvine, M., Berbigier, P., Nouvellon, Y., Dauzat, J., Taga, S., Hamel, O., Jourdan, C., Saint-André, L., Mialet-Serra, I., Labouisse, J.P., Epron, D., Joffre, R., Bra-connier, S., Rouzie're, A., Navarro, M., Bouillet, J.P., 2006. Partitioning energy and evapo-transpiration above and below a tropical palm canopy. Agr. Forest Meteorol. 139, 252–268.
- Roupsard O., van den Meersche K., Alline C., Rapidel B., Avelino J., et al., 2016. The "coffee-flux collaborative observatory": measuring and modeling carbon, nutrients, water and sediment Ecosystem services in a coffee agroforestry watershed (Costa Rica). 23 p. hal- 01837379. Available at https://hal.science/hal-01837379.
- Rutter, A., Kershaw, K., Robins, P., Morton, A., 1971. A predictive model of rainfall interception in forest. I. Derivation of the model from observation in a plantation of Corsican pine. Agricul. Meteorol. 9, 367–384.
- Schlesinger, W.H., Jasechko, S., 2014. Transpiration in the global water cycle. Agricul. For. Meteorol 189–190, 115–117. https://doi.org/10.1016/j.agrformet.2014.01.011.
- Schreiner-McGraw, A.P., Ajami, H., Anderson, R.G., Wang, D., 2022. Integrating partitioned evapotranspiration data into hydrologic models: vegetation parameterization and uncertainty quantification of simulated plant water use. Hydrol. Process. 36 (6), e14580. https://doi-org.ezproxy.princeton.edu/10.1002/hyn.14580
- Šimūnek, J., Šejna, M., Saito, H., Sakai, M., van Genuchten, M.T., 2013. The HYDRUS-1D Software Package For Simulating the One-Dimensional Movement of Water, Heat, and Multiple Solutes in Variably-Saturated Media (Version 4.17). Department of Environmental Sciences University of Riverside California, California.
- Siles, P., Harmand, J.M., Vaast, P., 2010. Effects of Inga densiflora on the microclimate of coffee (Coffea arabica L.) and overall biomass under optimal growing conditions in Costa Rica. Agrofor. Syst. 78, 269–286.

- Smith, A., Tetzlaff, D., Kleine, L., Maneta, M.P., Soulsby, C., 2021. Quantifying the effects of land-use and model scale on water partitioning and water ages using tracer-aided ecohydrological models. Hydrol. Earth Syst. Sci. https://doi.org/10.5194/hess-25-22391-2021
- Soetaert, K., Petzoldt, T., 2010. Inverse modelling, sensitivity and Monte Carlo analysis in R using package FME. J. Stat. Softw. 33, 01–28. https://doi.org/10.18637/jss. v033.i03
- Stevenson, J.L., Birkel, C., Comte, JC., et al., 2023. Quantifying heterogeneity in ecohydrological partitioning in urban green spaces through the integration of empirical and modelling approaches. Environ. Monit. Assess. 195, 468. https://doi. org/10.1007/s10661-023-11055-6.
- Tague, C., Band, L., 2004. RHESSys: regional Hydro-ecologic simulation system: an object-oriented approach to spatially distributed modeling of carbon, water and nutrient cycling. Ear. Interact. 8 (19), 1–42.
- Taugourdeau, S., et al., 2014. Leaf area index as an indicator of ecosystem services and management practices: an application for coffee agroforestry. Agric. Ecosyst. Environ, 192, 19–37
- te Wierik, S.A., Cammeraat, E.L.H., Gupta, J., Artzy-Randrup, Y.A., 2021. Reviewing the impact of land use and land-use change on moisture recycling and precipitation patterns. Water Resour. Res. 57, e2020WR029234, 2021.
- van Dijk, A., Bruijnzeel, L., 2001. Modelling rainfall interception by vegetation of variable density using an adapted analytical model, part 1. Model description. J. Hydrol. 247, 230–238.

- Van Griensven, A., Meixner, T., Grunwald, S., Bishop, T., Diluzio, M., Srinivasan, R., 2006. A global sensitivity analysis tool for the parameters of multi-variable catchment models. J. Hydrol. 324, 10–23.
- van Huijgevoort, M., Tetzlaff, D., Sutanudjaja, E., Soulsby, C., 2016. Using high resolution tracer data to constrain water storage, flux and age estimates in a spatially distributed rainfall–runoff model. Hydrol. Process. 30 (25), 4761–4778. https://doi. org/10.1002/hyp.10902.
- van Kanten, R., Vaast, P., 2006. Transpiration of arabica coffee and associated shade tree species in sub-optimal, low-altitude conditions of Costa Rica. Agrofor. Syst. 67, 187–202.
- Vaast, P., Bertrand, B., Perriot, J.J., Guyot, B., Génard, M., 2006. Fruit thinning and shade improve bean characteristics and beverage quality of coffee (coffea Arabica L.) under optimal conditions. J. Sci. Food Agric. 204, 197–204.
- Vezy, R., Christina, M., Roupsard, O., et al., 2018. Measuring and modelling energy partitioning in canopies of varying complexity using MAESPA model. Agr. For. Meteorol. 253–254, 203–217.
- Wohl, E., Barros, A., Brunsell, N., Chappell, N.A., Coe, M., Giambelluca, T., Goldsmith, S., Harmon, R., Hendrickx, J.M.H., Juvik, J., et al., 2012. The hydrology of the humid tropics. Nat. Clim. Chan. 2 (9), 655–662. https://doi.org/10.1038/nclimate1556.
- Zhang, X., et al., 2021. Greening-induced increase in evapotranspiration over Eurasia offset by CO2-induced vegetational stomatal closure. Environ. Res. Lett. 16, 124008 https://doi.org/10.1088/1748-9326/ac3532.
- Zhou, T., Nijssen, B., Gao, H., Lettenmaier, D.P., 2016. The contribution of reservoirs to global land surface water storage variations. J. Hydrometeorol. 17 (1), 309–325. https://doi.org/10.1175/JHM-D-15-0002.1, 2016.